Journal of Crystal Growth 310 (2008) 3121–3124

Contents lists available at ScienceDirect

Journal of Crystal Growth

journal homepage: www.elsevier.com/locate/jcrysgro

Microfluidic screening of potassium nitrate polymorphism

Philippe Laval, Céline Giroux, Jacques Leng, Jean-Baptiste Salmon *

LOF, unité mixte Rhodia-CNRS-Bordeaux 1, 178 avenue du Docteur Schweitzer, F-33608 Pessac cedex, France

ARTICLE INFO

Article history:
Received 7 December 2007
Received in revised form
3 March 2008
Accepted 6 March 2008
Communicated by R. Fornari
Available online 18 March 2008

Keywords:
A1. Nucleation
A1. Solubility
B3. Microfluidic devices

ABSTRACT

We developed a microfluidic device for the investigation of crystallization kinetics from solution. The device allows to store hundreds of ≈ 100 nL droplets containing a given solute and to control their temperature within 0.1 °C. Upon cooling, we observe independent and mononuclear crystallization events; crystal dissolution occurs as the temperature is raised. For potassium nitrate (KNO_3) in water, these thermal cycles reveal the existence of two concomitant polymorphic forms. We measured, for the first time, the solubility curves of both these polymorphs, defined unambiguously the metastability extent of the solution and described why these results essentially stem from the miniaturized scale of the crystallization reactors.

Polymorphism is the possibility of a given substance to crystallize in different structures. The prediction of which polymorph will crystallize is of high importance for both natural and laboratory (chemical, pharmaceutical,…) processes, since every single form displays specific properties [1–3]. However, there exists no comprehensive theory today to account for the complexity of the crystallization process from solution. This may be due to the interplay of the many parameters playing a relevant role in the process (pH, temperature, solvent…) but also to the experimental difficulties to access to the very early steps of nucleation [4–6]. Major recent breakthroughs concerning nucleation understanding were performed with numerical investigations on model systems [7,8], and with experimental studies on crystallization of colloidal particles and proteins [9,10].

High-throughput techniques that use microfluidics start bringing new insights via systematic and miniaturized screening of crystallization conditions [11–14]. These techniques require minute amount of material to allow for a large number of conditions to be tested. Of special interest is the specific control of the kinetic pathway followed in the phase diagram toward crystallization offered by the microfluidic environment [15–18]. Here, we present a microfluidic setup dedicated to the collection of thermodynamic and kinetic data on crystallization from aqueous solutions (Fig. 1). The setup is based on droplets formation and storage and allows to manipulate hundreds of droplets, each playing the role of an independent microreactor. Crystallization and dissolution in the drops are induced by cooling or warming up the chip. The high number of droplets yields a large sample of independent crystallization events, a prerequisite for statistical analysis of a stochastic process such as nucleation. Importantly, due to the small size of the droplets (≈ 100 nL), each crystallization event is mononuclear, i.e. involves a single nucleation event [19,20].

We use this device to characterize the crystallization of potassium nitrate in water. This inorganic compound displays a strong sensitivity to temperature and possesses several polymorphs, one of which showing ferroelectric properties with potential applications for memory storage [21,22]. With our device, we not only evidence the nucleation in solution of two polymorphs of KNO_3 around ambient conditions but also measure for the first time the two solubility curves and the metastability extent of the solubility curves with respect to the temperature.

1. Experimental procedure

The microfluidic device is fabricated in poly(dimethylsiloxane) (PDMS) using standard techniques [23]. The width and height of the channels are 500 μm. The PDMS device is sealed with a silicon wafer to maximize thermal transfers (Fig. 1(b) shows the same device sealed with a glass slide for clarity). Silicone oil (Rhodorsil 20 cSt) and the aqueous solution (KNO_3, Normapur Merck in deionized water) are injected at controlled flow rates using syringe pumps. Monodisperse aqueous droplets are formed at the intersection between the two streams [24,25]. Typical flow rates of 1800 and 600 μL/h for the oil and aqueous phases, respectively, produce droplets in the 100–200 nL range, the volume of the drops being determined by their formation frequency. Oil can also

* Corresponding author.
E-mail address: Jean-Baptiste.Salmon-exterieur@eu.rhodia.com (J.-B. Salmon).

0022-0248/$ - see front matter © 2008 Elsevier B.V. All rights reserved.
doi:10.1016/j.jcrysgro.2008.03.009

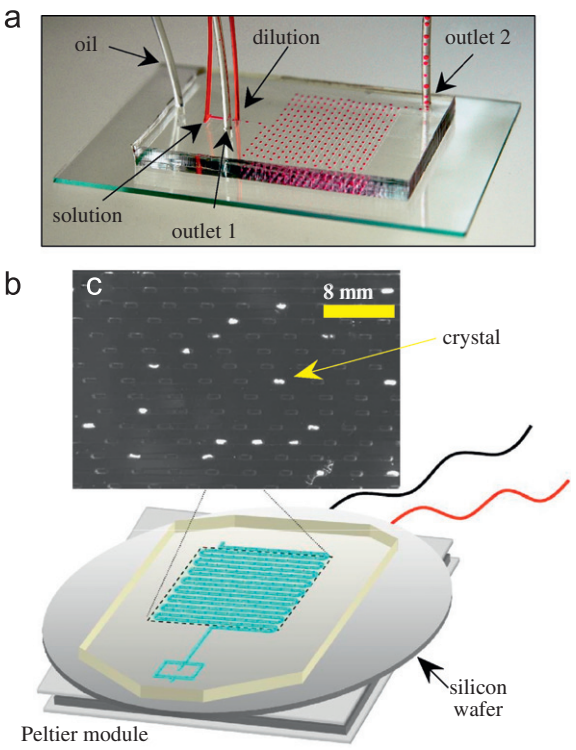

Fig. 1. (a) Picture of the microfluidic chip sealed on a glass slide (channel width and height: 500 μm). At the intersection between the oil and aqueous streams (solution), monodisperse droplets that here contain a colored dye are formed. Oil may also be injected after the droplet formation to move them apart (dilution). The droplets flow in the long microchannel when outlet 2 is opened and outlet 1 is closed while they are discarded (outlet 1) for the opposite. (b) Schematic setup: the PDMS device is sealed on a silicon wafer and placed on a Peltier module to control its temperature. (c) Image obtained under crossed polarizers of the storage area where birefringent crystals appear as bright spots.

be injected just after their formation (≈ 600 μL/h) to move the droplets apart and thus avoid their coalescence during storage (we do not use surfactants). Filling the device involves two steps: the stream of droplets is first directed in a storage serpentine (towards outlet 2, outlet 1 being closed); once the flow is steady, the two outlets are switched (outlet 1 is open, 2 is closed), thus leading to hundreds of droplets immobilized and stored in the long channel.

The temperature of the chip is controlled using a Peltier module (Melcor, $62 \times 62\,mm^2$) and a water circulation from a cryostat, both placed underneath the chip. The syringe containing the aqueous solution and the corresponding tubing need to be heated above the solubility temperature (with flexible heaters by Minco) and temperature is measured in the chip with thin thermocouples (80 μm of diameter, Thermocoax) inserted through the PDMS layer down to the silicon wafer. The large size of the Peltier module yields an uniform temperature field (within 0.1 °C) across the storage zone.

Images of the crystallization events in the droplets are taken using a stereo microscope equipped with a CCD camera. KNO_3 crystals are birefringent which permits a high contrast imaging under crossed polarizers (crystals appear as bright pixels on a dark background with a detectable size of about 100 μm at the magnification we use). Statistics on crystals are computed from image analysis using custom made programs. Crystals are characterized using optical microscopy and Raman spectroscopy performed in situ, in the chip and within the droplets, using a confocal microscope (LabRam HR/Jobin-Yvon excitation wavelength 532 nm, objective 10×).

2. Results and discussion

In a typical experiment, we prepare a sequence of microreactors and we then cycle the temperature to induce first crystallization and then total dissolution; such a kinetic route should provide the lower and the upper solubility limits. Here, we evidence two limits which correspond to the solubilities of two polymorphic KNO_3 forms.

The precise steps of the experiments are as follows: droplets of solution at a given concentration of KNO_3, are stored in the microdevice at a temperature above the solubility to avoid crystallization (during ≈ 10 min with ≈ 100 μL of solution consumed). After a fast quench to roughly 10 °C below the expected solubility, temperature is decreased slowly by steps of 1 °C, until all the droplets eventually contain crystals [see Fig. 2(a)]. We extract from image analysis, the fraction of droplets that contain a crystal against temperature. At a given and reproducible temperature $T_m \pm 1$ °C, crystals appear in almost all the reactors.

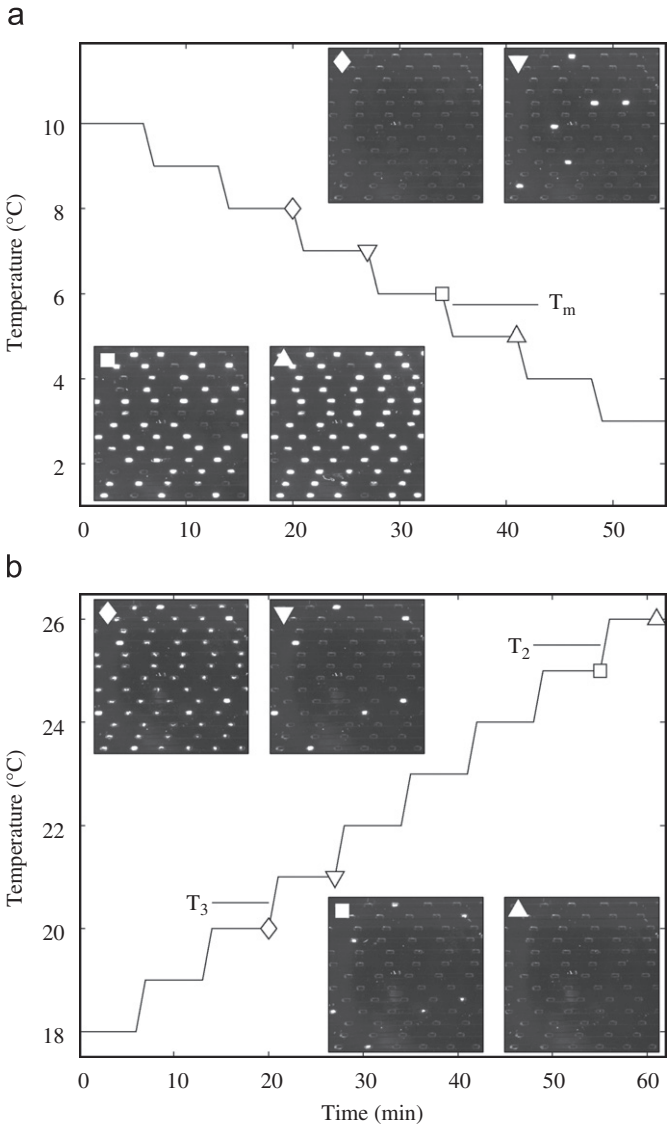

Fig. 2. Screening of crystallization temperature for one concentration ($c = 40\,g/100\,g$ of water). (a) Cooling ramp: T_m is the temperature at which most of drops contain crystals upon cooling (see text). (b) Heating ramp: dissolution of crystals happens in two steps (around T_3 and T_2), which corresponds to the solubility limits of two polymorphs of KNO_3.

When all the droplets contain a crystal, the temperature is raised by 1 °C steps. Typical images of the dissolution kinetics are shown in Fig. 2(b). At a given temperature T_3, most crystals have dissolved but a few do not until a higher temperature T_2 is reached. These two different dissolution temperatures suggest the occurrence of different polymorphs of the same crystal. We confirm this view using optical microscopy and Raman spectroscopy.

Microscopy not only reveals the specific crystallization habits of the different polymorphs (rough vs. faceted, inserts of Fig. 3), but also sheds light onto nucleation. We observed the bi-univocal correspondence between one droplet and one crystal and then we argued, as a first approximation, that only one nucleus formed in one droplet: because the growth kinetics is fast (a few seconds) compared to the mean induction time for nucleation (minutes to tens of minutes), the nucleation process is actually mononuclear [14,19]. The mononuclear nature of the crystallization events is a result of prime importance for the quantification we give below, and movies showing the nucleation inside droplets make this assessment obvious from visual inspection [26]. Once a nucleation event has occurred, the nucleus takes up all the solute from the solution and exhausts it, making any other nucleation event unlikely. Note, however, that when higher supersaturations are applied, more than once crystal may occur in drops, but we check it rarely happens in the experiments detailed here. While one of the two habits identified here involves a faceted crystal [Fig. 3(a)] which convincingly results from a singular event, the other crystal looks irregular and fragmented [Fig. 3(b)]. We nevertheless confirm that the latter also results from a mononuclear event; its rough aspect follows from the growth kinetics which is extremely rapid and may involve irregular shapes with many defects.

These different habits actually can be related to different crystalline structures: we selected the droplets according to the habit of their crystals and performed Raman spectroscopic measurements directly in situ, within the droplets. Thus, a definite identification of different structures is allowed (see Fig. 3): vibrational spectroscopy indeed shows that the two different looking crystals are characterized by different vibration modes and thus discriminates between several (tabulated) phases. The values of ν_1, ν_3, the vibration frequencies of the covalent modes of NO_3^- [27,28], allows us to identify the form which dissolves at T_2 as the stable form of KNO_3 (state II), and the ferroelectric form (state III) which dissolves at T_3 [21,22].

We thus unambiguously identified two polymorphs that may occur upon crystallization. Fig. 4 displays the variations of the measured temperatures T_m, T_3 and T_2 with the concentration c. T_m corresponds to an estimation of the metastability limit of the system for small volumes of reactors (100–200 nL). The values of T_m are of great importance for the optimization of a crystallization process (morphology, size, size distribution…). In our case, crystal nucleation has been systematically observed above T_m due to unavoidable impurities that are present in some drops, but they do not induce nucleation in others, as in a classical reactor by secondary nucleation. Therefore, the measured values of T_m are closer to that of homogeneous nucleation [19]. T_2 vs. c corresponds to the solubility curve of KNO_3 found in the literature (state II) [29]. However, the curve T_3 vs. c indicates the presence of the metastable state III whose solubility is higher than that of the stable state at a given temperature. Using our device, we have observed the nucleation *in solution* of this metastable form, and measured its solubility. To our knowledge, the solubility of this metastable form has never been measured previously.

The reasons making these measurements possible are manifold, yet they stem from the miniaturization: reactors are small

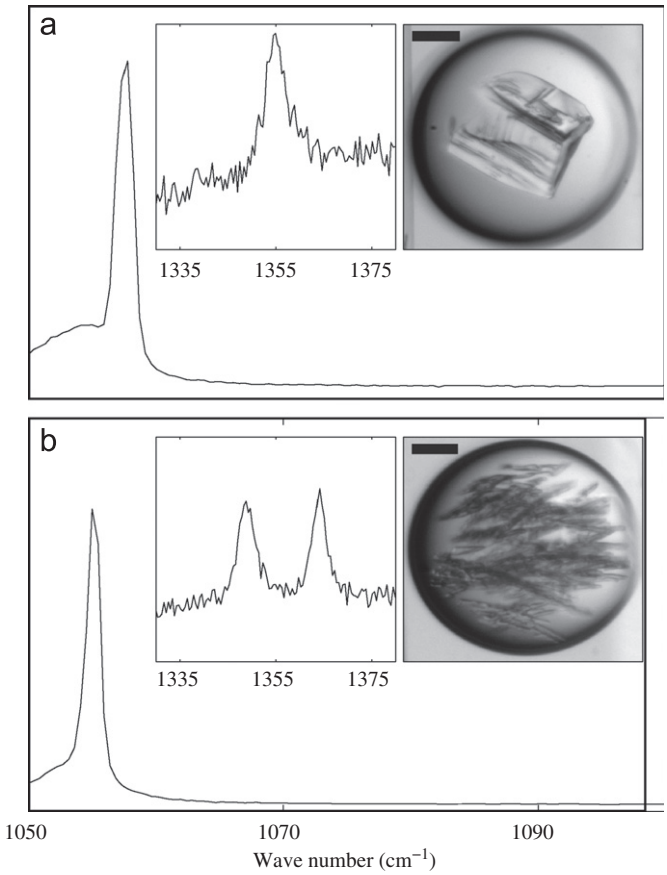

Fig. 3. Raman spectra measured on the two different crystals. (a) State III that dissolves at T_3, (b) state II at T_2. Stretching mode ν_1 of NO_3^- at (a) 1058, (b) 1055 cm^{-1}. Inserts: Raman bands of ν_3 modes, at (a) 1355 cm^{-1}, and (b) 1348 and 1364 cm^{-1}; and corresponding habits observed in the droplets (scale bars = 100 μm).

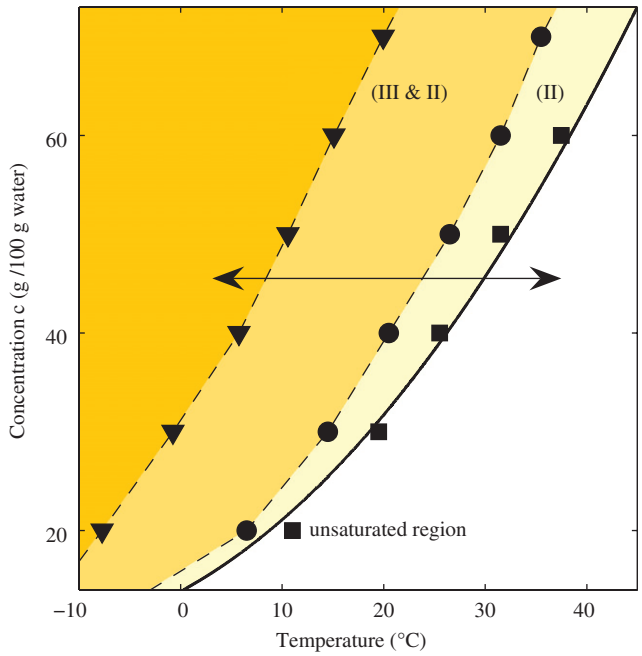

Fig. 4. (•) and (■) are the dissolution curves for KNO_3 measured with the microfluidic device and correspond to T_3 and T_2, respectively. The black line is an interpolation of solubility data found in the literature [29], others are guides for the eyes. (▼) correspond to the temperatures T_m where almost all the crystals appear in the droplets.

enough to yield mononuclear crystallization at (possibly) high supersaturation. In a classical reactor, polymorphic transitions occur when the different crystals coexist, and it is thus difficult to characterize the metastable form that may dissolve rapidly. In our case, we overcome this problem, because we observe independent crystals that have grown after mononuclear nucleation. Moreover, since the involved volumes are small, higher supersaturations can be reached that may promote nucleation of metastable polymorphs. One other advantage of the droplets with respect to macroscopic systems, is that only volume and surface diffusions are allowed between solution and crystals, whilst the convective movements, that accelerate the kinetics (both for nucleation and growth), are hindered. This probably affects the possibility of observing the metastable phases in small systems, because the rate of their transformation in the stable ones is decreased. We also measure the dissolution of a large number of individual crystals, thus revealing more easily the solubility of the different polymorphs. Besides, the ease to implement analytical tools such as Raman measurements constitutes another decisive advantage. The accurate temperature control ($<0.1\,^{\circ}C$) permits to distinguish polymorphic forms with close solubilities, and the low amount of consumed liquid in a given experiment ($<100\,\mu L$) is also of great interest for studies on expensive solutions. For all the above reasons, we believe that our setup may be a useful tool for screening new polymorphic forms, especially when their difference in Gibbs free energy is small and, particularly, in the field of pharmaceutical research.

Acknowledgments

We gratefully thank M. Joanicot and A. Ajdari for fruitful discussions and acknowledge Région Aquitaine for funding and support.

References

[1] J. Bernstein, J. Phys. D: Appl. Phys. 26 (1993) 66.
[2] K. Sato, J. Phys. D: Appl. Phys. 26 (1993) 77.
[3] J. Bernstein, R.J. Davey, J.-O. Henck, Angew. Chem. Int. Ed. 38 (1999) 3440.
[4] J.W. Mullin, Crystallization, Butterworth-Heinemann, Oxford, 2001.
[5] A.C. Zettlemoyer, Nucleation, Marcel Dekker, New York, 1969.
[6] N. Rodriguez-Hornedo, D. Murphy, J. Pharmaceut. Sci. 88 (1999) 651.
[7] P.R. ten Wolde, D. Frenkel, Science 277 (1997) 1975.
[8] C. Desgranges, J. Delhommelle, Phys. Rev. Lett. 98 (2007) 235502.
[9] U. Gasser, E.R. Weeks, A. Schofield, P.N. Pusey, D.A. Weitz, Science 292 (2001) 258.
[10] O. Gliko, N. Neumaier, W. Pan, I. Haase, M. Fischer, A. Bacher, S. Weinkauf, P.G. Vekilov, J. Am. Chem. Soc. 127 (2005) 3433.
[11] C.L. Hansen, E. Skordalakes, J.M. Berger, S.R. Quake, Proc. Natl. Acad. Sci. USA 99 (2002) 16531.
[12] K. Shinohara, T. Fukui, H. Abe, N. Sekimura, K. Okamoto, Langmuir 22 (2006) 6477.
[13] B. Zheng, J.D. Tice, L.S. Roach, R.F. Ismagilov, Angew. Chem. Int. Ed. 43 (2004) 2508.
[14] P. Laval, J.-B. Salmon, M. Joanicot, J. Crystal Growth 303 (2007) 622.
[15] C.L. Hansen, S. Classen, J.M. Berger, S.R. Quake, J. Am. Chem. Soc. 128 (2006) 3142.
[16] J. Leng, B. Lonetti, P. Tabeling, M. Joanicot, A. Ajdari, Phys. Rev. Lett. 96 (2006) 084503.
[17] C.J. Gerdts, V. Tereshko, M.K. Yadav, I. Dementieva, F. Collart, A. Joachimiak, R.C. Stevens, P. Kuhn, A. Kossiakoff, R.F. Ismagilov, Angew. Chem. Int. Ed. 45 (2006) 8156.
[18] J. Shim, G. Cristobal, D.R. Link, T. Thorsen, Y. Jia, K. Piattelli, S. Fraden, J. Am. Chem. Soc. 129 (2007) 8825.
[19] D. Kashchiev, D. Clausse, C. Jolivet-Dalmazzone, J. Colloid Interface Sci. 165 (1994) 148.
[20] D. Kashchiev, G.M. van Rosmalen, Crystal Res. Technol. 38 (2003) 555.
[21] F.C. Kracek, J. Phys. Chem. 34 (1930) 225.
[22] J.K. Nimmo, B.W. Lucas, Acta Crystallogr. B32 (1976) 1968.
[23] J.C. Mcdonald, G.M. Whitesides, Accounts Chem. Res. 35 (2002) 491.
[24] T. Thorsen, F.H. Roberts, F.H. Arnold, S.R. Quake, Phys. Rev. Lett. 86 (2001) 4163.
[25] S.L. Anna, N. Bontoux, H.A. Stone, Appl. Phys. Lett. 82 (2003) 364.
[26] Movie showing the nucleation inside droplets can be found at ⟨www.lof.cnrs.fr/article.php3?id_article=163⟩.
[27] M. Balkanski, M.K. Teng, M. Nusimovici, Phys. Rev. 176 (1968) 1098.
[28] M.H. Brooker, J. Phys. Chem. Solids 39 (1978) 657.
[29] D.R. Lide, Handbook of Chemistry and Physics, CRC Press, 2004–2005.